Seismic Response Analysis of Seismically Isolated Buildings using Observed Records due to 2011 Tohoku Earthquake

Mineo Takayama & Keiko Morita
Fukuoka University, Japan

SUMMARY:
The Great East Japan Earthquake that occurred in 2011 caused serious damage to a widespread area. The human damage and number of buildings drowned out by the tsunami were great, and there were many cases where old buildings were damaged by the shock of the earthquake. However, most seismic isolated buildings were not severely damaged and fully showed the effect of their performance. The large ground motions caused by this earthquake that hit across a wide stretched area, from the Kanto area to the Tohoku area, lasted for a longer period of time than any of the past. The effects that long-duration earthquake ground motions have on the response of seismic isolated buildings and the characteristics of seismic isolated devices were verified by a seismic response analysis of seismic isolated buildings. Furthermore, a comparison with the earthquake motions that had been observed inland of Japan verified the characteristics of Tohoku earthquake.

Keywords: Seismic Isolation, Response Analysis, Earthquake

1. INTRODUCTION

In Japan, more than 2600 seismically isolated buildings have been constructed. The seismic isolation technology has been applied to office buildings, condominiums, hospitals and detached houses. In order to obtain the optimum isolation effect, various devices (rubber bearing, sliding bearing, roller bearing, hysteresis damper, oil damper, etc.) are used in combination.

After 1995 Kobe earthquake, National Research Institute for Earth Science and Disaster Prevention (NIED) deploys the digital strong-motion seismograph (K-net & Kik-net) across the all of Japan. The collected seismic data analyses are made available to the public on the Internet. On 11 March 2011, Great East Japan Earthquake (Tohoku Earthquake) occurred. After the main shock, several earthquakes occurred. The main shock was recorded at more than 900 stations of K-net & Kik-net.

The observed maximum acceleration during the Tohoku Earthquake was 2.7G in horizontal direction and 1.8G in vertical direction. The duration time of the observed records was much longer than the near fault earthquake such as Kobe earthquake. In the Tohoku region hardest hit by this earthquake, there were many seismic isolated buildings. Almost all seismic isolated buildings were safe and show their performance. The response of seismic isolated building was estimated by dynamic response analysis using the observed records.

In this paper, the observed earthquake records of seismic isolated buildings were introduced. The response of seismic isolated buildings due to the observed earthquake records was studied in comparison with the response of the buildings caused by earthquakes in the past, such as 1995 Kobe earthquake, 2004 Niigata earthquake, etc.

2. OBSERVED EARTHQUAKE RECORDS

The number of seismic isolated buildings has been increasing dramatically, since the 1995 Great Hanshin-Awaji Disaster (Kobe earthquake). The number of detached houses with seismic isolation has been increasing from 2000 due to the revised standard of buildings. Figure 1 shows the number of buildings with seismic isolation. The first seismic isolated building was built in 1982. After Kobe earthquake, the number of isolated buildings increased dramatically and has been maintained at around 170 buildings each year. Half of them are apartment house. Remarkably, almost all hospitals which have been built after 1995 have a seismic isolation system.

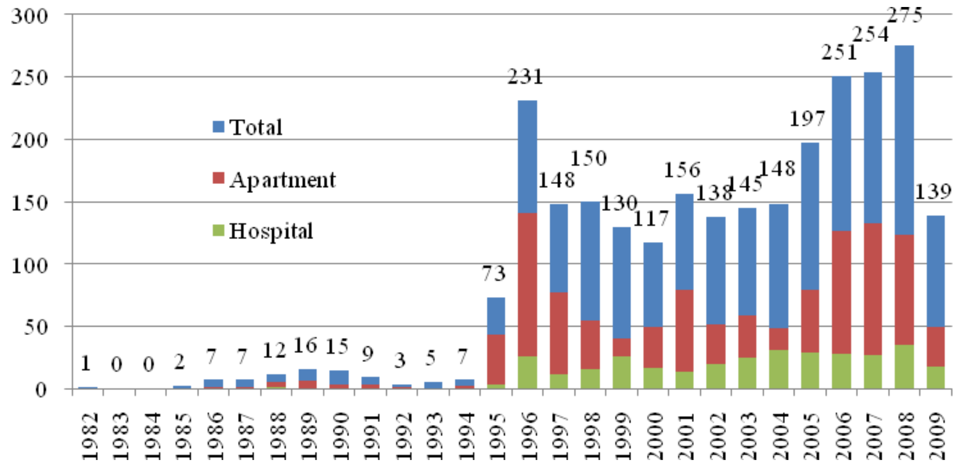

Figure 1 Number of Seismic Isolated Buildings in Japan (the detached houses are not included)

Table 1 shows part of the observed earthquake records of 27 seismic isolated buildings during the 2011 Tohoku Earthquake. The table shows the use of buildings, isolation systems, the maximum acceleration observed, and the maximum deformation of the seismic isolation layer measured (a Blank space indicates no measurement). The types of buildings include an office, a hospital, an apartment, a school etc. and the stories of the buildings vary from 2 to 36. Among the isolation systems used there, there are simple systems using only high-damping rubber or lead rubber bearing. Also, there are isolation systems combined with sliding bearing and various types of damper along with laminated rubber bearing. In every case, the most optimum system was selected in order to achieve the seismic isolation performance, which was the goal of the design.

The maximum acceleration obtained in these buildings was 756 gal, which was recorded in a seismic isolated building of two stories in Fukushima Pref. The maximum deformation of the seismic isolation layer was more than 20 cm in the Tohoku districts of Miyagi Pref. and Fukushima Pref., and they were less than 10 cm in the Kanto Districts of Tokyo and Chiba pref. The deformation of a seismic isolation layer of more than 40 cm was observed in a three-story building in Miyagi Pref, which is not shown in this table. At any rate, it was revealed that seismic isolated buildings fully showed the effect of their performance.

Figure 2 shows the maximum response accelerations observed in seismic isolated buildings. The horizontal axis of this figure shows the maximum acceleration at the basement of the seismic isolation layer, and the vertical axis shows the ratio of the maximum accelerations (amplification factors) of the 1st floor (1FL) and the highest floor (Top floor) against that of the basement of the seismic isolation layer. From all observed results, it is revealed that the accelerations of the superstructure were more greatly damped than those of the basement (input acceleration) and that the larger the escalation of the basement, the greater the effect of seismic isolation becomes. But the amplification factor is greater than 1.0 when the input acceleration is small.

Table 1 Observed Earthquale Records of Sesimic Isolated Buildings during 2011 Tohoku Earthquake

Prefecture	Use	Story	Isolation System	Max. Acceleration (gal)			Max. Displacement of Isolation Floor (cm)
				Base	1st Floor	Top Floor	
Aomori	Office	10	LRB	104	122	123	2
Iwate	Hospital	6	NRB+LRB+SLB+SD	305	83	183	9
Miyagi	House	2	SLB	508	185		26
	Office	5	HDR	345	177	224	11
	Office	6	HDR	381	200	209	18
	Office	9	HDR+OIL	289	121	142	18
	Office	18	NRB+SLB	311	173	194	23
Fukushima	Office	2	NRB+LRB+SLB+OIL	756	213	155	24
	Office	3	LRB+SLB+OIL	411	184	154	
Ibaragi	Research Lab	3	NRB+SD+LD	296		121	6
	Research Lab	5	NRB+LD	305	238	203	19
	Office	7	NRB+LRB+SD	327	92	126	6
	Apartment	21	NRB+SD+LD	402	185	181	15
Chiba	Apartment	4	LRB	170	101	107	3
	Apartment	4	HDR	169	149	139	5
	Office	8	NRB+HDR	219	97.5	137	5
Tokyo	Research Lab	2	NRB+SD	143	113	120	4
	Apartment	3	NRB+OIL	90	54	90	5
	Museum	4	HDR	100	76	100	4
	Office	4	NRB+SLB	95	75	75	3
	Research Lab	6	LRB	132	69	72	9
	Office	11	NRB+LRB+OIL	104	55	94	5
	Apartment	12	NRB+LRB	100	53	61	7
	Cram School	26	NRB+OIL	98	29	46	9
	Apartment	36	NRB+LRB	129	100	116	15
Kanagawa	School	7	NRB+OIL	71	54	57	12
	School	7	HDR	147	51	99	7

NRB: Natural Rubber Bearing, HDR: High Damping Rubber Bearing,
LRB: Lead Rubber Bearing, SLB: Sliding Bearing
OIL: Oil Damper, SD: Steel Damper, LD: Lead Damper

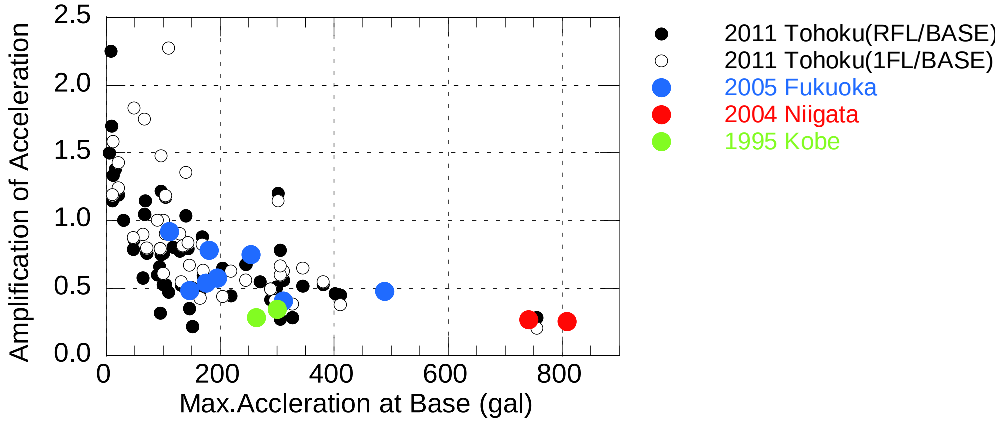

Figure 2 Amplification Factor of Observed Acceleration of Seismic Isolated Buildings

3. RESPONSE ANALYSIS

3.1. Characteristics of Observed Earthquake Records

National Research Institute for Earth Science and Disaster Prevention (NIED) deploys the digital strong-motion seismograph (K-net & Kik-net) across the all of Japan. The collected seismic data analyses are made available to the public on the Internet. On 11 March 2011, Tohoku Earthquake occurred. After the main shock, several earthquakes occurred. The main shock was recorded at more than 900 stations of K-net & Kik-net. Table 2 shows the peak acceleration at 7 stations including the station recorded the maximum acceleration (station code: MYG004) among the main shock. At the several stations, the peck acceleration was over 1G.

Table 2 Maximum Acceleration Records due to Tohoku Earthquake (unit: gal)

Prefecture	Station Code	Location	NS-dir.	EW-dir.	UD-dir.
Miyagi	MYG004	Tsukidate	2699.9	1268.5	1879.9
	MYG010	Ishinomaki	458.2	377.0	332.0
	MYG013	Sendai	1517.2	982.3	290.2
	MYG015	Iwanuma	410.7	353.2	253.9
	MYGH10	Yamamoto	870.8	852.7	622.2
Tochigi	TCG006	Ogawa	377.6	376.1	181.2
Fukushima	FKS020	Inawashiro	241.5	275.6	96.0

Figure 3 shows the acceleration wave observed at MYG004 station. The envelope of that wave is unusual. The main shock occurred 2 times due to this earthquake. The duration time is much longer than the near fault earthquake such as Kobe earthquake.

Figure 4 shows the response spectra of observed waves shown in Table 2. There are three response spectra of: velocity spectrum (5% damping), energy spectrum (10% damping) and displacement spectrum (20% damping). The energy spectrum was proposed by Akiyama(1985), which can be obtained by earthquake energy input into elastic vibration system of 10% damping being calculated. The vertical axis of (b) of the figure shows the energy input by earthquake being converted into equivalent velocity by Eqn. 3.4. The displacement spectrum is calculated presuming a 20% equivalent damping constant of seismic isolated buildings.

The MYG004 wave that recorded the largest acceleration among the observed waves showed a very high response in the neighborhood of a 0.2 second period, but it showed smaller responses than other observed waves for more than 1 second periods. In velocity spectrum and energy spectrum, the MYG010 wave and TCG006 wave showed high responses at more than 1 second periods. In the displacement spectrum, these waves showed high responses exceeding 30 cm in the range of from a 2 second period to a 4 second period, and the MYG015 wave showed the highest response. Following these, the FKS020 wave also showed a high displacement response. This is because the observation point of the FKS020 wave was on soft ground, so that the observed wave included many long-period components.

Before 2011 Tohoku Earthquake, several earthquakes had resulted in damage to buildings, such as the 1994 Northridge Earthquake, the 1995 Kobe Earthquake, the 2004 Niigata Chuetsu Earthquake, the 2007 Chuetsu-Oki Earthquake, and the 2008 Iwate-Miyagi Inland Earthquake. Figure 5 shows the response spectra by observed waves of these earthquakes. Although the earthquake motions shown here were of short duration, the maximum velocities were over 100 cm/s. The velocity spectra exceeded 200 cm/s in the range of from a 1 second period to near a 3 second period, and some of them exceeded 400 cm/s at the maximum. The displacement spectra with a damping ratio of 20% showed the response of over 40 cm at more than 2 second periods, and those of large earthquake waves exceeded 60 cm. The design displacement of many seismic isolated buildings designed in Japan is around 40 cm, and the clearance up to the retaining wall is often around 60 cm. In the case where these strong earthquake motions are input, it will become necessary to presume situations such as collision to the retaining wall, fracturing of laminated rubber bearing, etc. It is revealed that the maximum response deformation of the seismic isolated buildings during the 2011 Tohoku Earthquake was small compared with the response by these earthquake motions

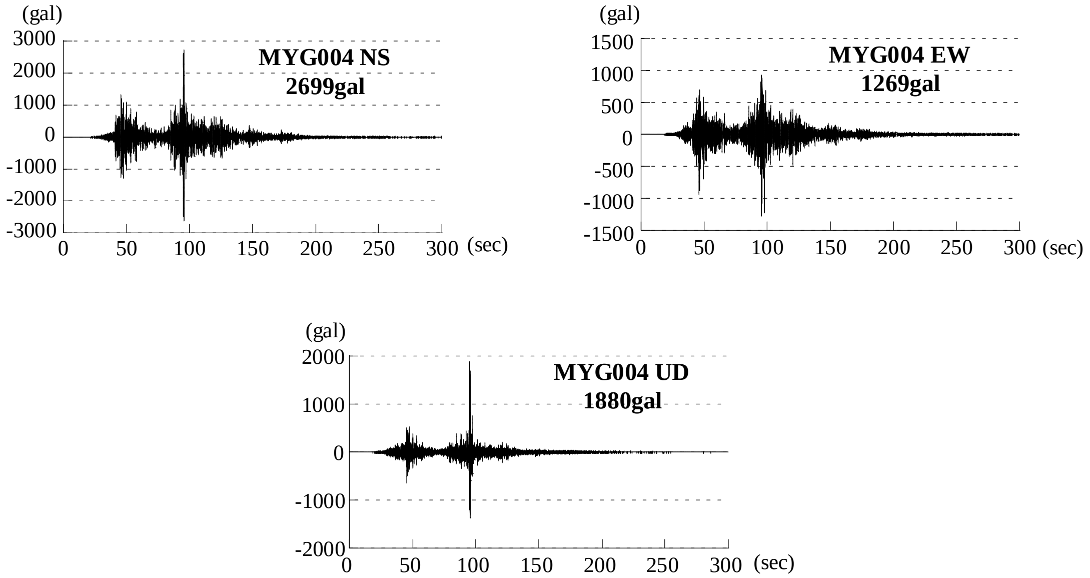

Figure 3 Acceleration Records of MYG004

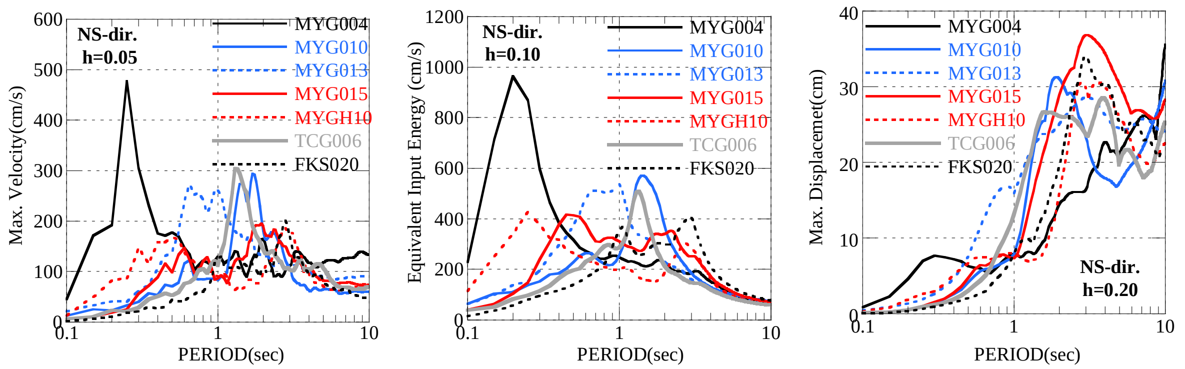

(a)Velocity Spectrum (5% Damping) (b)Energy Spectrum (10%) (c)Displacement Spectrum (20%)

Figure 4 Response Spectra of 2011 Tohoku Earthquake

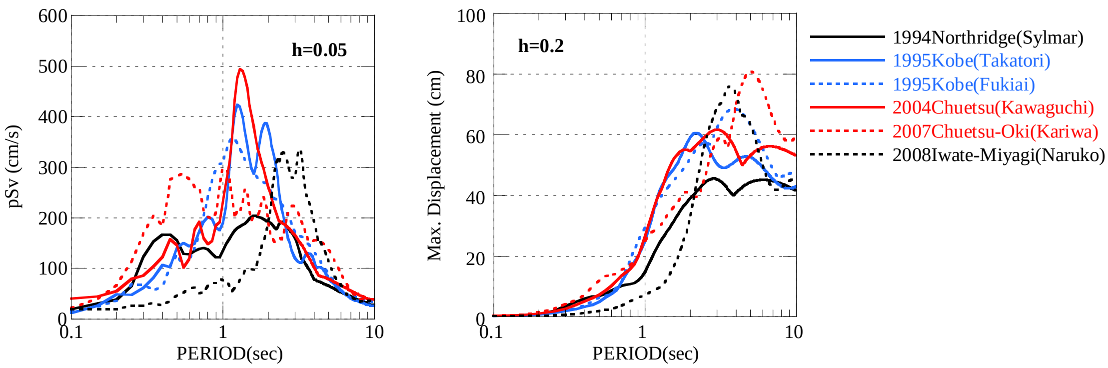

(a)Velocity Spectrum (5% Damping) (b)Displacement Spectrum (20%)

Figure 5 Response Spectra of Near fault Earthquake

3.2. Response Analysis of Seismic Isolated Buildings

3.2.1. Analytical model

The analytical model used was a single-degree-of-freedom model, and the characteristic of the seismic isolation layer was presumed to be restoring force characteristics of bi-linear type, as shown in Figure 6. Viscous damping was not taken into account. The seismic isolation period, T_d, and yield shear coefficient, α_s, in Eqn. 3.5 are important factors for the response evaluation of seismic isolation buildings. The seismic isolation period here was presumed as the period based upon the stiffness after yield, and it was varied in the range of from approximately 1 sec. to 10 sec. The yield shear coefficient is the rate of yield load against the total mass of a building, and its range was presumed to be 0.02-0.05. The yield displacement was presumed as constant at 1 cm.

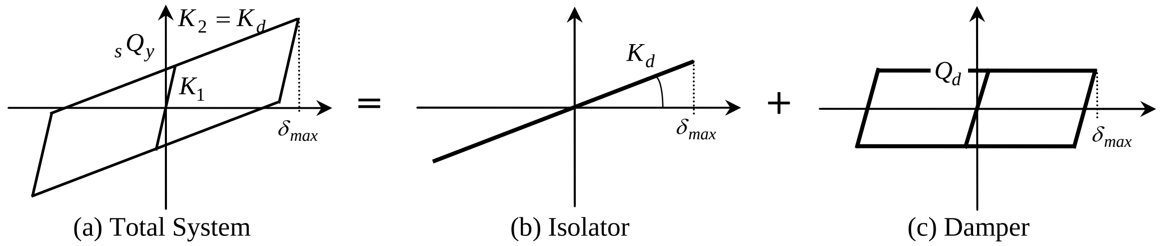

Figure 6 Restoring Force Characteristic of Analytical Model

3.2.2. Response prediction by energy balance

It can be presumed that seismic isolation layers of seismic isolated building can absorb all earthquake input energy. The characteristics of seismic isolation layers are presumed to be able to be shown in the bi-linear type as shown in Figure 6. Eqn. 3.1 was obtained as energy equilibrium equation in seismic isolation layer.

$$W_e + W_p = E \tag{3.1}$$

W_e of Eqn. 3.1 is the elastic vibration energy, and it is obtained in Eqn. 3.2 as the energy absorbed by the linear spring (Isolator) K_d shown in Figure 6(b). δ_{max} is the maximum displacement of seismic isolation layer.

$$W_e = \frac{1}{2} K_d \delta_{max}^2 \tag{3.2}$$

W_p is the elasto-plastic strain energy, which is equivalent to the absorbed energy by the entire elasto-plastic spring (damper) as shown in Figure 6(c). If the yield load and accumulated plastic deformation of damper are Q_d and δ_p, respectively, Eqn. 3.3 is obtained.

$$W_p = Q_d \delta_p \tag{3.3}$$

The energy input E of the earthquake is converted to the equivalent velocity V_E by Eqn. 3.4.

$$E = \frac{MV_E^2}{2} \tag{3.4}$$

Substitute Eqn. 3.2 to 3.4 to Eqn. 3.1 and sort out it with Eqn. 3.5, then Eqn. 3.6 is obtained.

$$T_d = 2\pi \sqrt{\frac{M}{K_d}} \quad , \quad \alpha_s = \frac{Q_d}{Mg} \tag{3.5}$$

where, M : the total mass of building, g : the acceleration of gravity

$$\alpha_1 = \frac{15\pi^2 \delta_{max}}{4gT_d^2} + \frac{V_E^2}{16g\delta_{max}} \tag{3.6}$$

Figure 7 shows the relationship between the sear coefficient α_1 and maximum displacement $\delta_{\max}$

obtained by Eqn. 3.6. The seismic isolation period here was 4 seconds. This reveals that, if the equivalent velocity of earthquake input energy is constant, a response prediction curve becomes convex in the downward direction, and there is a minimum point of response. The response of a seismic isolation building becomes larger along with larger earthquake input energy. When the equivalent velocity of earthquake input energy is 200 cm/s, the maximum response displacement is approximately 30 cm. However, when the equivalent velocity becomes 400 cm/s, the response displacement becomes larger, up to approximately 50 cm. The red straight lines in the figure show the horizontal stiffness corresponding to the 4 second seismic isolation period. The shorter the seismic isolation period is, the steeper the inclination of the lines becomes. It is important to establish the optimum seismic isolation period corresponding to the equivalent velocity of earthquake input energy and the yield shear coefficient of a damper. The responses that are predicted by this method tend to show the value on the safe side, i.e., larger than the results of the time history response analysis.

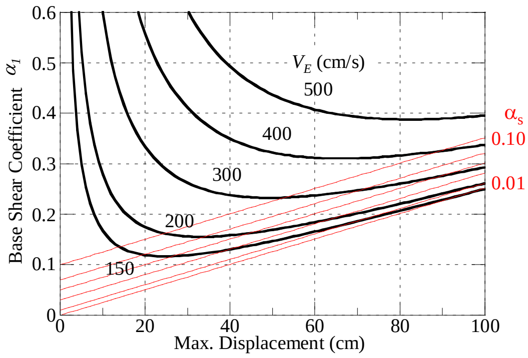

Figure 7 Response Prediction by Energy Balance (T_d =4sec)

3.2.3. Analytical results

The results of seismic response analysis of seismic isolation buildings are shown in Figures 8, 9 and 10. Figure 8 shows the maximum response displacement of seismic isolation layers, Figure 9 the accumulated displacements, and Figure 10 the maximum shear coefficients. The horizontal axis of each graph shows the seismic isolation period, and the yield shear coefficient, α_s, of a damper shows the three cases of 0.02, 0.03 and 0.05. The reason why responses are large at the periods of less than 2 seconds is that, because the periods are short, the hysteresis damping is small. In the cases where the seismic isolation period is more than 4 seconds, the maximum response displacement and accumulated displacement are stable. When the damping is small (α_s is small), the responses of the MYGH10 wave and FKS020 wave become large in the neighborhood of a 3 second period. However, their peaks become smaller with larger α_s.

The maximum response displacements of the MYG015 wave and MYG013 wave were largest at around 40 cm. The MYG004 wave, which showed a very large response value in the range of short periods in the velocity response spectrum (Figure 4), shows the maximum displacement at approximately 20 cm. Through all the analytical results, the maximum displacements of approximately 50 cm are shown at the periods of about three seconds, but the maximum displacements become approximately 40 cm at periods of more than 4 seconds.

Accumulated displacement is related to the energy absorption capacity of a damper, so that it provides an indication of evaluating energy absorption capacity. The longer the seismic isolation period is, the smaller the accumulate displacement becomes. The accumulated displace is 30 m at the maximum in the neighborhood of a 3 second seismic isolation period, and it is reduced to around 10 m if the period becomes longer. There are large differences according to the kinds of earthquake wave, too. The MYG010 wave does not largely change, caused by the yield shear coefficient, α_s, of a damper, and shows approximately 10 m at periods of more than 3 second seismic isolation periods.

The longer the seismic isolation period is, the more the maximum yield shear coefficient of seismic isolation layer reduces, and the larger the yield shear coefficient becomes, the larger the maximum yield shear coefficient of seismic isolation layer becomes. The shear coefficient falls below 0.1 when the seismic isolation period is over 4 seconds. In order to reduce the shear coefficient when the seismic isolation period is short, it may be necessary to add an oil damper, etc.

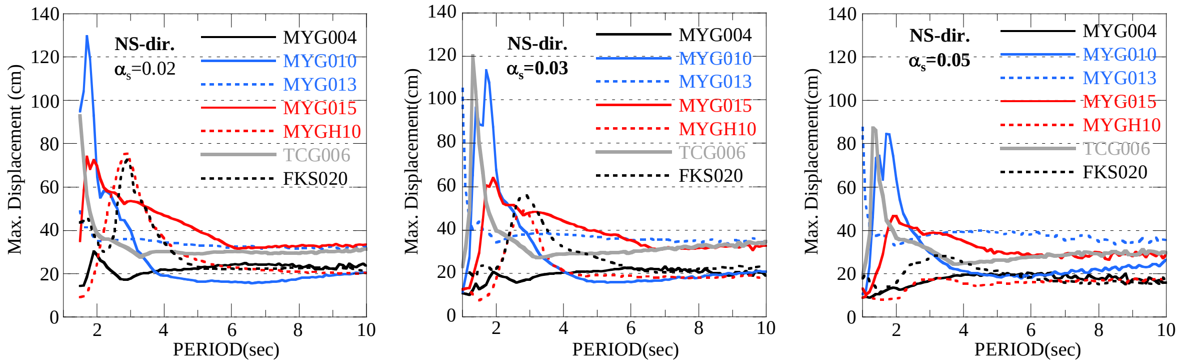

(a) α_s =0.02 (b) α_s =0.03 (c) α_s =0.05

Figure 8 Maximum Response Displacement

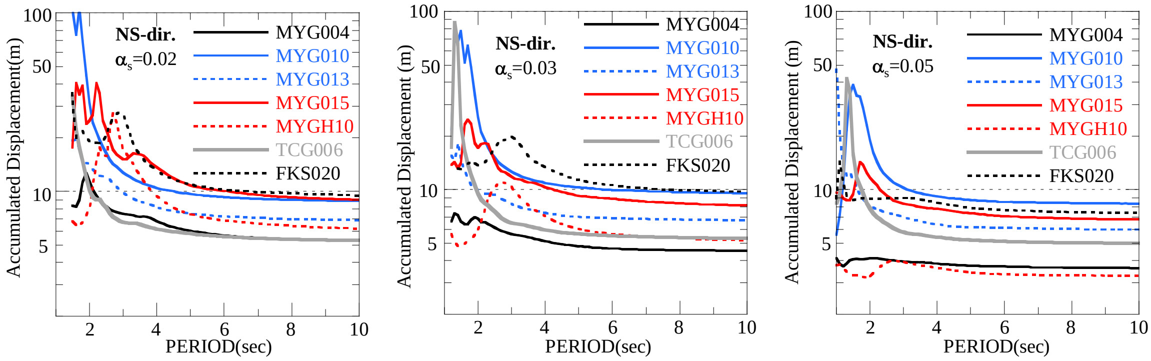

(a) α_s =0.02 (b) α_s =0.03 (c) α_s =0.05

Figure 9 Accumulated Displacement

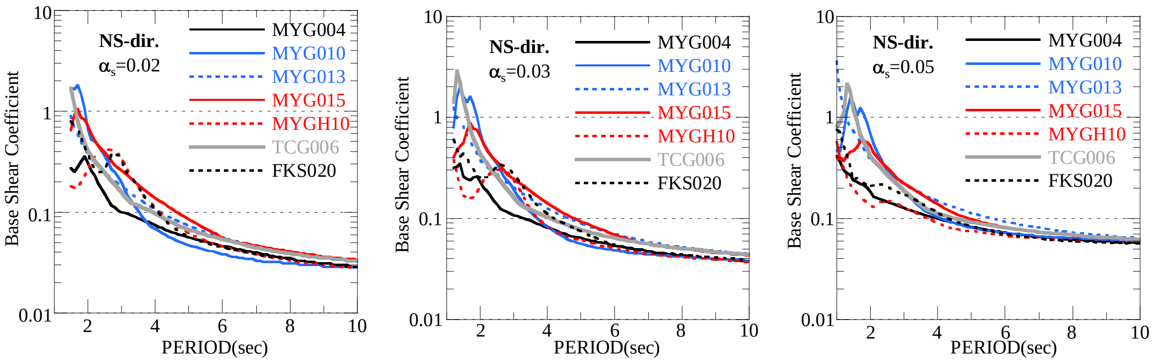

(a) α_s =0.02 (b) α_s =0.03 (c) α_s =0.05

Figure 10 Base Shear Coefficient

4. EXAMINATION OF RESIDUAL PERFORMANCE

The responses of seismic isolation buildings were shown in the previous clause, for which the observation records obtained from the 2011 Tohoku Earthquake were used. It is presumed that the maximum response displacement of seismic isolation buildings was approximately 40 cm, and accumulated displacements were in the range from 10 m to 20 m. If the accumulated displacement becomes larger, naturally the earthquake energy absorbed by the isolation system increases. The earthquake energy absorbed ultimately becomes heat. It is important to verify to what extent the isolation system can absorb earthquake energy.

Figure 11 shows the results of the experiments, which were repeated many times, for lead rubber bearing, which was proposed by Takayama et al.(2008). The experiments were repeated 200-times under the condition shear strain being 200% and excited frequency at 0.33Hz. The hysteresis loop of (a) of the figure shows that the yield load comes down with increases in the number of repetitions. (b) of the figure shows the accumulated displacement and the variation of yield load, Q_d , and horizontal stiffness, K_d . From this figure, the horizontal stiffness almost does not come down, but the yield load goes down by half when the accumulated displacement is less than 10 m. This is the effect of the generation of heat of the lead plug inserted to the center of the laminated rubber.

In the seismic response analysis, it was presumed that the accumulated displacement was more than 10 m, and the yield load of laminated rubber containing the lead plug is considered to go down to some extent. It is presumed that the maximum response displacement also increases with decreases in the yield load.

For the actual prediction of earthquake response, the reduction of yield load caused by the generation of heat like this should be taken into consideration.

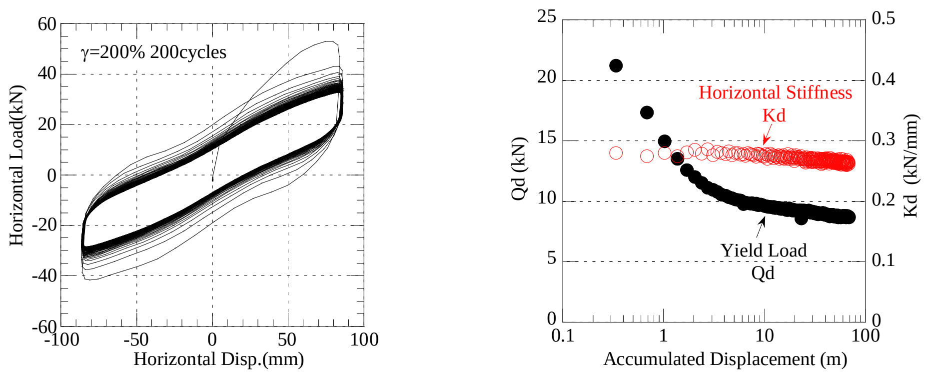

(a)Hysteresis Loop (b)Variation of Yield Load and Stiffness

Figure 11 Experimental Results of LRB

5. CONCLUSIONS

In this paper, the seismic response analyses of seismic isolation buildings were implemented using the earthquake waves that were considered to greatly affect the seismic isolation buildings from many records observed from the 2011 Tohoku Earthquake. Also, the earthquake waves were compared with those observed in the past.

The maximum response displacement of seismic isolation buildings caused by 2011 Tohoku Earthquake is considered to 30 cm-40 cm, and this is consistent with the records obtained from the earthquake observation. Compared with the earthquake observation records of the past, the duration time of the earthquake wave of this earthquake was long and many aftershocks followed, so that many repeated deformations affected the isolation systems. It is necessary to verify the energy absorption capacity of seismic isolation devices. In some seismic isolation devices, the yield load decreases and the energy absorption capacity deteriorates along with repeated deformation. Therefore, it is required to properly take such characteristics into account at the structural design stage.

AKCNOWLEDGEMENT

We would like to express our appreciation to all people involved to help us in our study. We were provided the observed data of seismic isolated buildings by Japan Society of Seismic Isolation and these committee members.

REFERENCES

Akiyama Hiroshi (1985), Earthquake-Resistant Limit-State Design for Buildings, University of Tokyo Press.

Takayama M, Kousaka R., Kikuchi T. (2008). Durability of Rubber Isolators by Long-Duration Ground Motion due to Large Earthquakes, *14th World Conference on Earthquake Engineering*, Beijing, China 2008